Electron and hole g factors measured by spin-flip Raman scattering in $CdTe/Cd_{1-x}Mg_xTe$ single quantum wells

A. A. Sirenko,* T. Ruf, and M. Cardona
Max-Planck-Institut für Festkörperforschung, Heisenbergstrasse 1, D-70569 Stuttgart, Germany

D. R. Yakovlev,* W. Ossau, A. Waag, and G. Landwehr
Physikalisches Institut der Universität Würzburg, Am Hubland, D-97074 Würzburg, Germany

(Received 4 March 1997)

We report resonant spin-flip Raman scattering measurements in $CdTe/Cd_{1-x}Mg_xTe$ single quantum wells with $x=0.15$, 0.26, and 0.5 as well as in $Cd_{1-x}Mg_xTe$ alloys with $x=0$, 0.15, and 0.5. Effective g factors of electrons and heavy holes are measured as a function of the quantum well width (18−100 Å) and the angle of the magnetic field with respect to the growth axis. The electron g factors in quantum wells are between the values for bulk CdTe ($g^e=-1.644\pm0.005$) and $Cd_{0.85}Mg_{0.15}Te$ ($g^e=-0.802\pm0.005$). We show that the change in the energy gap induced by the quantum confinement of the carriers provides the dominant contribution to the electron g factor in quantum wells. A large g factor anisotropy for conduction electrons is observed. It is shown that this anisotropy depends on the splitting between light- and heavy-hole states. The experimentally determined g factors are in good agreement with theoretical predictions.
[S0163-1829(97)06128-6]

I. INTRODUCTION

Electron and hole g factors are among the fundamental properties of charge carriers in semiconductors. The effective electron g factor can differ strongly from its value in vacuum due to the spin-orbit coupling. The g factors are directly related to semiconductor band parameters.[1,2] A precise knowledge of g factors is important for the interpretation of phenomena such as magneto-optics, magnetotransport, resonance spectroscopy on spin-split sublevels, and light scattering.[3,4]

Recently, the carrier g factors in low-dimensional systems have attracted the interest of both theorists[5–8] and experimentalists.[9–20] In heterostructures and quantum wells (QW's) the g factors of electrons and holes often deviate from the bulk values. Several reasons can be adduced to explain these differences in zinc-blende based structures:

(i) The band parameters are changed by the confinement, especially the energy gap.

(ii) The reduced symmetry of the system results in an anisotropy of the *electron* g factor.[5] As a consequence it might become important to take off-diagonal components of the electronic g factor tensor into account (for more details see Refs. 7,8).

(iii) Carrier wave functions penetrate into the barrier material resulting in different contributions to the g factor.

(iv) Strain effects due to the lattice mismatch between the dissimilar materials in heterostructures may be important. Combinations of these reasons, which depend distinctly on the structure parameters (like, e.g., the QW width), cause in low-dimensional systems a rather complicated behavior of the g factors on such parameters.

Various experimental techniques have been applied to study carrier g factors in QW's.[9] A remarkable anisotropy of the electron g factor has been observed in $Ga_{1-x}In_xAs/InP$ QW's by optically detected magnetic resonance,[10] and in $GaAs/Al_{1-x}Ga_xAs$ QWs under optical orientation of electron spins.[11–13] It has also been *directly* measured in GaAs/AlAs QW's by resonant spin-flip Raman scattering (SFRS).[14] Nevertheless, the experimental data base for electron and hole g factors in low-dimensional systems is far from complete and at present is limited predominantly to heterostructures based on the III-V semiconductors. Only very recently g factors in wide (80–300 Å) II-VI semiconductor QW's ($CdTe/Cd_{0.75}Mg_{0.25}Te$) have been measured by means of quantum beat spectroscopy and photoluminescence (PL).[15]

In this paper we study g factors of excitons, electrons, and heavy holes in $CdTe/Cd_{1-x}Mg_xTe$ single quantum wells (SQW's) with the aim to determine the dominant systematics of their values and anisotropy. We use resonant SFRS, which has been shown to be one of the most reliable experimental techniques for a direct measurement of g factors in low-dimensional systems such as $GaAs/Al_{1-x}Ga_xAs$ QW's,[14,16–18] submonolayer InAs/GaAs structures,[19] and structures with $InP/In_{1-x}Ga_xP$ quantum dots.[20]

II. EXPERIMENT

$CdTe/Cd_{1-x}Mg_xTe$ heterostructures with the type-*I* band alignment were grown by molecular-beam epitaxy on (001)-oriented CdTe and $Cd_{0.97}Zn_{0.03}Te$ substrates (for growth details see Refs. 21,22). The CdTe SQW's with widths L_W between 18 Å and 100 Å are confined between $Cd_{1-x}Mg_xTe$ barriers with $x=0.15$, 0.26, and 0.5. The structures were not intentionally doped. The residual concentration of shallow impurities does not exceed $10^{15}-10^{16}$ cm^{-3}. The parameters of the structures are given in Table I. The SFRS experiments were carried out in magnetic fields B up to 14 T at a temperature of 5 K. The experimental setup allows us to vary the angle between the magnetic field and the growth axis of the structure (z axis) from 0° to 90°. The SFRS

TABLE I. The electron, exciton and heavy-hole g factors and structural parameters of the CdTe/$Cd_{1-x}Mg_x$Te SQW's with different QW width L_W. The heavy-hole g factor components are determined using the relationship: $g^{hh}=g^{ex}+g^e$. For all measured structures $g_\perp^{ex}=-g_\perp^e$ is valid and, consequently, $g_\perp^{hh}=0.00\pm0.04$. g_{PL}^{ex} is the exciton g factor determined from the Zeeman splitting of the PL lines. Note the difference in the error bars between SFRS and PL data. The splitting between the light- and heavy-hole states $\Delta E_{lh\text{-}hh}$ has been measured by PLE.

L_W (Å)	x	E_{ex} (eV)	$\Delta E_{lh\text{-}hh}$ (meV)	$g_\parallel^e$	$g_\perp^e$	$g_\parallel^{ex}$	g_{PL}^{ex}	$g_\parallel^{hh}$
18	0.15	1.751	26.1	-1.04 ± 0.01	-0.95 ± 0.01	2.71 ± 0.03	2.6 ± 0.3	1.67 ± 0.04
45	0.15	1.663	24.5	-1.36 ± 0.01	-1.23 ± 0.01	2.20 ± 0.03	2.1 ± 0.3	0.84 ± 0.04
60	0.15	1.641	20	-1.44 ± 0.01	-1.32 ± 0.01	2.04 ± 0.03	1.8 ± 0.3	0.60 ± 0.04
100	0.15	1.612	12.5	-1.59 ± 0.01	-1.49 ± 0.01	1.59 ± 0.03	1.6 ± 0.3	0.00 ± 0.04
75	0.26	1.633	16.5	-1.46 ± 0.01	-1.37 ± 0.01	1.46 ± 0.03	1.6 ± 0.3	0.00 ± 0.04
70	0.50	1.657	37	-1.37 ± 0.01	-1.15 ± 0.01	1.52 ± 0.03	1.3 ± 0.3	0.15 ± 0.04

spectra were analyzed with a SPEX 1404 double monochromator equipped with a cooled GaAs photomultiplier. A tunable Ti-sapphire laser was used for resonant excitation of heavy-hole excitons.

The PL and photoluminescence excitation (PLE) spectra in these CdTe/$Cd_{1-x}Mg_x$Te QW's have been systematically studied.[22–24] A high structural quality of the interfaces (the fluctuations of L_W do not exceed one monolayer) and an effective confinement of both carrier types in the CdTe wells (the valence band offset is equal to about 30% of the total band-gap difference) have been established.[22] The lattice mismatch between zinc-blende MgTe and CdTe is 1.0% ($a_{CdTe}=6.4825$ Å and $a_{MgTe}=6.417$ Å).[21] The PL spectra are dominated by the heavy-hole exciton localized on QW width fluctuations and the exciton bound to shallow donors.[24] The energies of the heavy-hole exciton transition E_{ex} for our samples, determined from PLE, are given in Table I. The light-hole and heavy-hole states in the CdTe/$Cd_{1-x}Mg_x$Te SQW's are split due to both, confinement and stress caused by the lattice mismatch between the barrier and the well material.[22] These two effects act in the same direction for our system and push the light-hole state to higher energies. The splitting between the light- and heavy-hole states $\Delta E_{lh\text{-}hh}$, determined from PLE, is included in Table I.

III. RESULTS AND DISCUSSION

In magnetic fields we observed narrow Stokes and anti-Stokes SFRS lines for excitation in resonance with the heavy-hole exciton transition. SFRS spectra were measured with crossed circular polarizations: (σ^+,σ^-) and (σ^-,σ^+) for the Stokes and anti-Stokes parts of the spectra, respectively. Here the first (second) symbol corresponds to the polarization of the exciting (backscattered) light. The solid line in Fig. 1 shows the Stokes part of a SFRS spectrum for $\mathbf{B}\|\mathbf{z}$. The lines EX and E have been attributed to exciton and electron spin-flip processes, respectively.[16,19] The electron line is narrow and its full width at half maximum (FWHM) is limited by that of the laser line (L). The exciton line is broadened due to the hole contribution. This is common for SFRS spectra in QW's (see, e.g., Ref. 14).

As shown in Fig. 2 the spin-flip shifts of the exciton and electron lines, Δ^{ex} and Δ^e, are directly proportional to the magnetic field. The linear dependence of $\Delta^{ex}(B)$ shows that the mixing between light- and heavy-hole states is weak up to 14 T. This is expected because the requirement $\Delta^{ex}\ll\Delta E_{lh\text{-}hh}$ is always fulfilled for all our samples (Δ^{ex} is about 1 meV at $B=10$ T, $\Delta E_{lh\text{-}hh}>10$ meV). A nonlinear behavior for exciton Zeeman splittings was reported in Ref. 25 for wide GaAs/AlGaAs QW's, where $\Delta E_{lh\text{-}hh}$ is considerably smaller. On the other hand the magnetic fields used in our experiments are strong enough to break up the spin-dependent electron-hole exchange interaction. The exchange splitting of the fourfold degenerate exciton levels at $B=0$ is

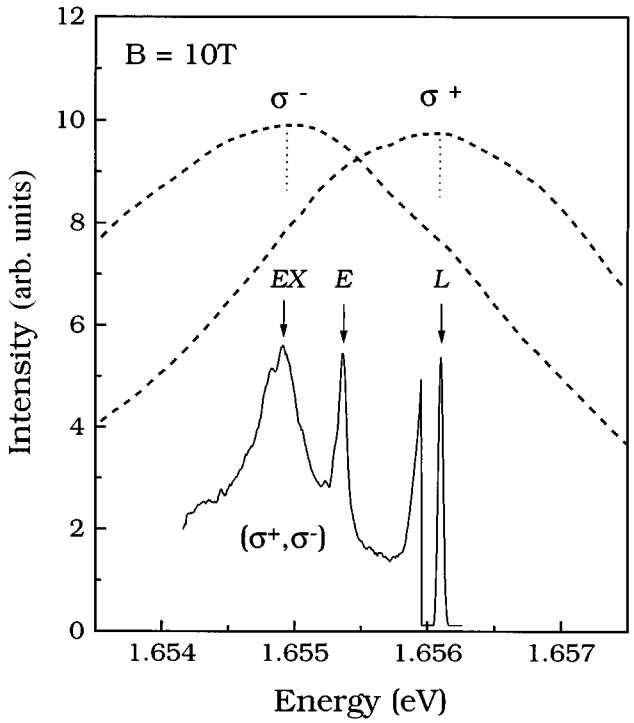

FIG. 1. SFRS (solid line) and PL (dashed lines) spectra of a 45 Å CdTe/$Cd_{0.85}Mg_{0.15}$Te SQW at $B=10$ T ($\mathbf{B}\|\mathbf{z}$). The SFRS spectrum has been measured in the crossed circular polarizations (σ^+,σ^-), where the first (second) symbol corresponds to the polarization of the exciting (scattered) light. Exciton and electron spin-flip lines, and laser line (attenuated by a neutral density filter) are marked with EX, E, and L, respectively. σ^+ and σ^- are the circular polarizations of the exciton components in the PL spectra.

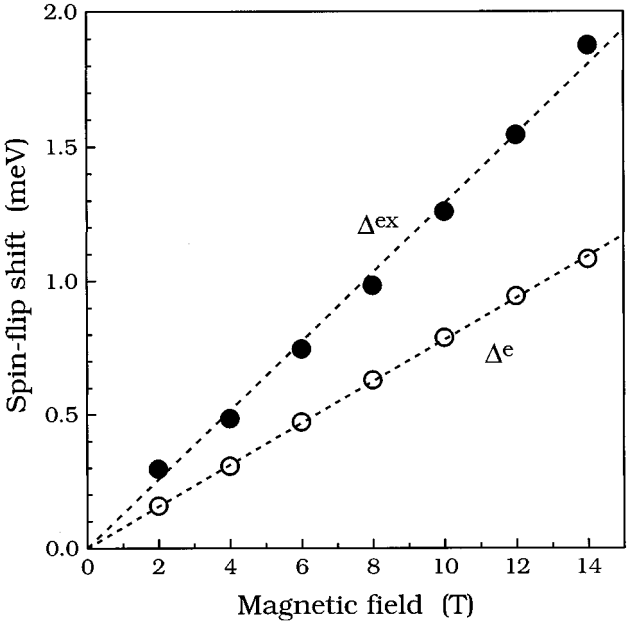

FIG. 2. Exciton and electron spin-flip shifts, Δ^{ex} and Δ^{e}, in a 45 Å $CdTe/Cd_{0.85}Mg_{0.15}Te$ SQW vs. magnetic field applied at 15° to the QW axis. The dashed straight lines are guides to the eyes.

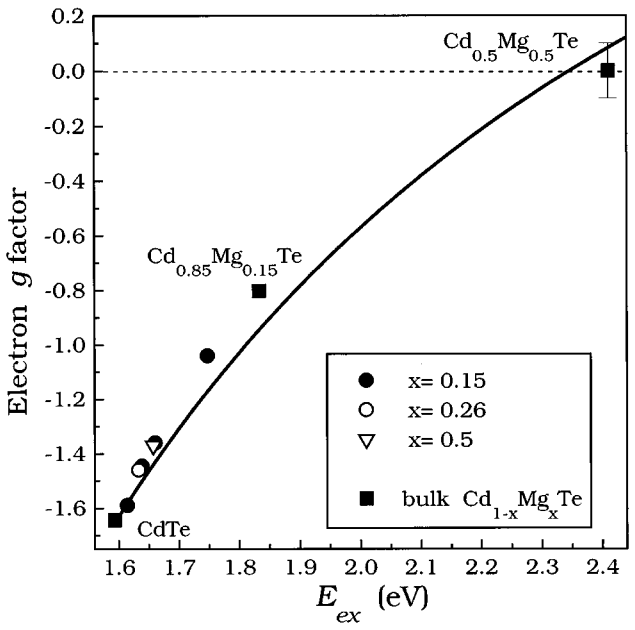

FIG. 3. Dependence of the longitudinal component of the electron g factor $g_{\parallel}^{e}$ on the energy of the heavy-hole exciton transition E_{ex} for $CdTe/Cd_{1-x}Mg_xTe$ SQW's. The solid line represents a five-band $\mathbf{k}\cdot\mathbf{p}$ calculation according to Eq. (1). The g factors for bulk $Cd_{1-x}Mg_xTe$ are shown by squares.

supposedly small compared to Zeeman splittings and can be disregarded here. Thus, Δ^{ex} can be considered as the Zeeman splitting between optically allowed states of the heavy-hole exciton for $\mathbf{B}\|\mathbf{z}$.[19] Δ^{e} corresponds to the electron component in the Zeeman splitting of the heavy-hole exciton. Δ^{ex} and Δ^{e} can be related to the *absolute* values of the exciton and electron g factor components along the growth direction, $g_{\parallel}^{ex}$ and $g_{\parallel}^{e}$, by the relationship $\Delta^{ex,(e)}=|g_{\parallel}^{ex,(e)}|\mu_B B$, where μ_B is the Bohr magneton ($\mu_B \simeq 0.05788$ meV/T).

We discuss next the signs of the electron and exciton g factors in CdTe-based QW's. A *positive* sign of $g_{\parallel}^{ex}$ was determined experimentally from the selection rules for circular polarization of the corresponding Raman lines.[16,19] A negative sign of $g_{\parallel}^{e}$ was determined experimentally for the sample with $L_W=18$ Å, where a heavy-hole spin-flip line was also detected. The negative sign of $g_{\parallel}^{e}$ corresponds to a larger spin-flip shift for the exciton line than for the heavy-hole line Δ^{hh}: $\Delta^{ex}>\Delta^{hh}$. Since it is known that bulk CdTe has a negative electron g factor,[2,26] we have taken a *negative* sign of $g_{\parallel}^{e}$ for all QW's studied. Thus, in our experiments the electron and exciton g factors are measured directly. The heavy-hole g factor $g_{\parallel}^{hh}$ is determined by the relationship: $g_{\parallel}^{hh}=g_{\parallel}^{ex}+g_{\parallel}^{e}$. The g factor values are summarized in Table I for samples with different L_W. Similar data for wider QW's (100−300 Å) have been obtained from spin quantum beats.[15]

The exciton g factor can also be obtained from the Zeeman splitting dE of the optically allowed circularly polarized (σ^+ and σ^-) components in the PL spectrum[15] such as those shown by the dashed lines in Fig. 1. We measured dE for $\mathbf{B}\|\mathbf{z}$ and determined the exciton g factor g_{PL}^{ex} from $dE=E^{\sigma^+}-E^{\sigma^-}=g_{PL}^{ex}\mu_B B$. The exciton g factors determined by SFRS agree within the experimental accuracy with the ones measured from the PL line splitting for all our samples (see Table I). However, the SFRS data have a much higher accuracy due to the narrower FWHM. This demonstrates the advantage of SFRS in comparison with conventional PL measurements for systems where the inhomogeneous broadening of the PL spectrum exceeds considerably the Zeeman splittings.

In the following we will first concentrate on the electron g factor. Figure 3 shows experimental values for $g_{\parallel}^{e}$ vs. the heavy-hole exciton energy for the samples with different L_W and Mg contents in the barriers. Data for bulk $Cd_{1-x}Mg_xTe$ alloys are represented by squares. The values determined for $g_{\parallel}^{e}$ fall in the range between the electron g factor measured for bulk CdTe ($g^e=-1.644\pm0.005$) and the barrier material $Cd_{0.85}Mg_{0.15}Te$ ($g^e=-0.802\pm0.005$). The increase in $g_{\parallel}^{e}$ with E_{ex} can be understood by using the five-band $\mathbf{k}\cdot\mathbf{p}$ model.[27,28] In this approximation confinement effects are taken into account via the changes in E_{ex} only. Relatively small variations of $g_{\parallel}^{e}-g_0$ ($g_0=2$ is the free electron Landé factor) are expected since both, the gap and spin-orbit splitting change rather little with the confinement. For the analysis of $g_{\parallel}^{e}(E_{ex})$ the value of $\Delta E_{lh\text{-}hh}$ is neglected in comparison with E_{ex} (this is valid since our samples have typical values of $\Delta E_{lh-hh}/E_{ex}\approx 0.01$). The solid line in Fig. 3 corresponds to the following expression:[1,2]

$$g_{\parallel}^{e}(E_{ex})\approx g_0\left[1-\frac{E_P}{3}\left(\frac{1}{E_{ex}}-\frac{1}{E_{ex}+\Delta_0}\right)-\frac{E_P'}{3}\left(\frac{1}{E(\Gamma_7^c)-E_{ex}}-\frac{1}{E(\Gamma_8^c)-E_{ex}}\right)+C'+\frac{2}{9}\frac{\sqrt{E_P E_P'}\Delta^-}{E(\Gamma_7^c)-E_{ex}}\left(\frac{1}{E_{ex}}+\frac{2}{E_{ex}+\Delta_0}\right)\right], \qquad (1)$$

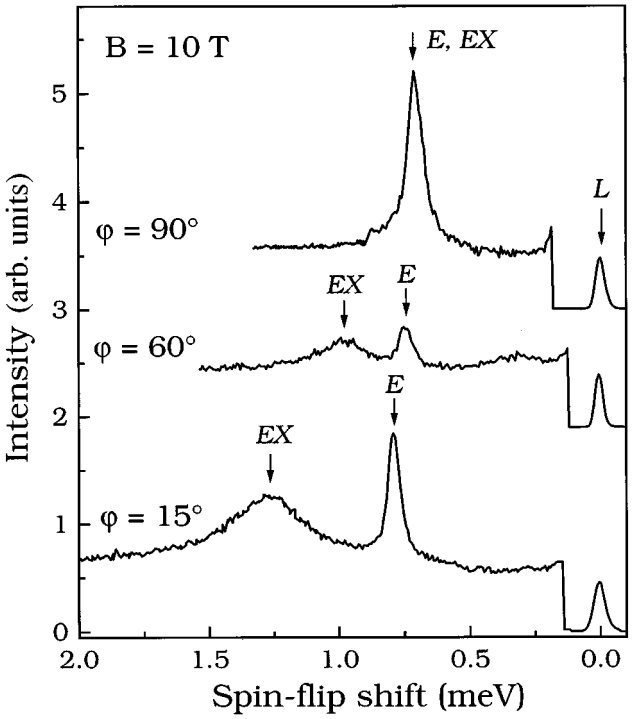

FIG. 4. SFRS spectra for a 45 Å $CdTe/Cd_{0.85}Mg_{0.15}Te$ SQW at $B=10$ T and different angles φ between **B** and **z**. The notation used for the spin-flip lines is the same as in Fig. 1.

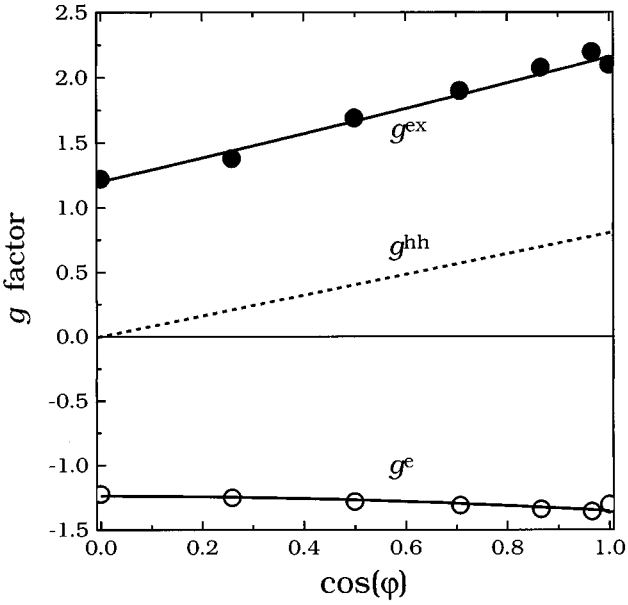

FIG. 5. Exciton and electron g factors, g^{ex} and g^e, vs. the angle φ between the magnetic field and the structure axis for the 45 Å $CdTe/Cd_{0.85}Mg_{0.15}Te$ SQW. The solid lines are fits using Eqs. (2) and (3). The angular dependence of the heavy-hole g factor g^{hh} is taken as a sum of g^{ex} and g^e (dashed line).

where the band parameters[1,2,28] $E_P=21.0$ eV, $\Delta_0=0.93$ eV, $E_P'=5.1$ eV, $E(\Gamma_8^c)=5.6$ eV, $E(\Gamma_7^c)=5.3$ eV, $C'=-0.02$, and $\Delta^-=-0.16$ eV are taken to be the same as for bulk CdTe. The good agreement between the experimental data and the calculation leads to the conclusion that the variation of the electron g factor in $CdTe/Cd_{1-x}Mg_xTe$ QW's with changing structural parameters (QW width and barrier content) is determined by the confinement effect on the energy gap, i.e., by E_{ex}.

Let us consider next the situation when the magnetic field is tilted by an angle φ with respect to the QW growth axis. SFRS spectra taken for different values of φ are presented in Fig. 4. Note that the electron line E depends only weakly on φ, whereas the exciton line EX shifts significantly and reaches the position of E at $\varphi = 90°$. Figure 5 shows the experimental values of g^{ex} and g^e as a function of $\cos\varphi$ for the sample with $L_W=45$ Å. The lines represent fits using the common expressions for the components of electron and heavy-hole g factor tensors:

$$g^e(\varphi)=-\sqrt{(g_\parallel^e\cos\varphi)^2+(g_\perp^e\sin\varphi)^2}, \tag{2}$$

$$g^{\mathrm{ex}}(\varphi)=\sqrt{(g_\parallel^e\cos\varphi)^2+(g_\perp^e\sin\varphi)^2}+\sqrt{(g_\parallel^{\mathrm{hh}}\cos\varphi)^2+(g_\perp^{\mathrm{hh}}\sin\varphi)^2}, \tag{3}$$

with the parameters $g_\parallel^e=-1.36\pm0.01$, $g_\perp^e=-1.23\pm0.01$, $g_\parallel^{\mathrm{hh}}=0.84\pm0.04$, and $g_\perp^{\mathrm{hh}}=0\pm0.04$, which are the longitudinal ($\mathbf{B}\|\mathbf{z}$) and transverse ($\mathbf{B}\perp\mathbf{z}$) components of the electron and the heavy-hole g factors, respectively. The dotted line, corresponding to the heavy-hole g factor, is the sum of $g^e(\varphi)$ and $g^{ex}(\varphi)$ calculated from Eqs. (2) and (3). Values for $g_{\parallel,\perp}^{e,\mathrm{hh}}$ are listed in Table I. For all measured structures we found $g_\perp^{ex}=-g_\perp^e$ and, therefore, $g_\perp^{\mathrm{hh}}=0.00\pm0.04$.

The anisotropy of the electron g factor in a 60-Å-thick QW is shown in more detail in the inset of Fig. 6, where the dashed line is calculated from Eq. (2) with parameters given in Table I. Note that the anisotropies of the electron and heavy-hole g factors have different reasons. That of g^e is determined by the reduction of the point symmetry from T_d (bulk) to D_{2d} (QW's) resulting in a splitting between light- and heavy-hole states,[5] whereas the anisotropy of the heavy-hole g factor corresponds to the symmetry of the periodic part of the Bloch functions of the heavy-hole state, which are expected to be nearly the same in QW's and in bulk zinc-blende semiconductors: $|g_\parallel^{\mathrm{hh}}|\gg|g_\perp^{\mathrm{hh}}|\approx0$.[29] The splitting between light- and heavy-hole states correlates with the electron g factor anisotropy Δg, defined as $\Delta g\equiv g_\perp^e-g_\parallel^e$. Figure 6 shows the dependence of Δg on $\Delta E_{\mathrm{lh\text{-}hh}}$ in the different structures. Δg is *positive* in all SQW's studied and becomes larger with increasing $\Delta E_{\mathrm{lh\text{-}hh}}$. This is illustrated by the values of Δg observed for two samples with close values of L_W (75 Å and 70 Å) but with a different Mg content in the barrier materials ($x=0.26$ and 0.5, respectively). Due to the different strain of the QW-layer the values of $\Delta E_{\mathrm{lh\text{-}hh}}$ are 16.5 and 37 meV, respectively. Consequently, the anisotropy of the electron g factor is also different: 0.09 and 0.22, respectively (see the open symbols in Fig. 6). This trend in the dependence of Δg on $\Delta E_{\mathrm{lh\text{-}hh}}$ can be illustrated using a simple two-band $\mathbf{k}\cdot\mathbf{p}$ approximation for the Γ_6^c and Γ_8^v bands, by analogy with the case of a uniaxial crystal.[28] The contribution to the electron g factor from other bands ($\Gamma_7^v,\Gamma_7^c,\Gamma_8^c$) should be almost isotropic and can be neglected here. The solid line in Fig. 6 corresponds to the following qualitative expression:

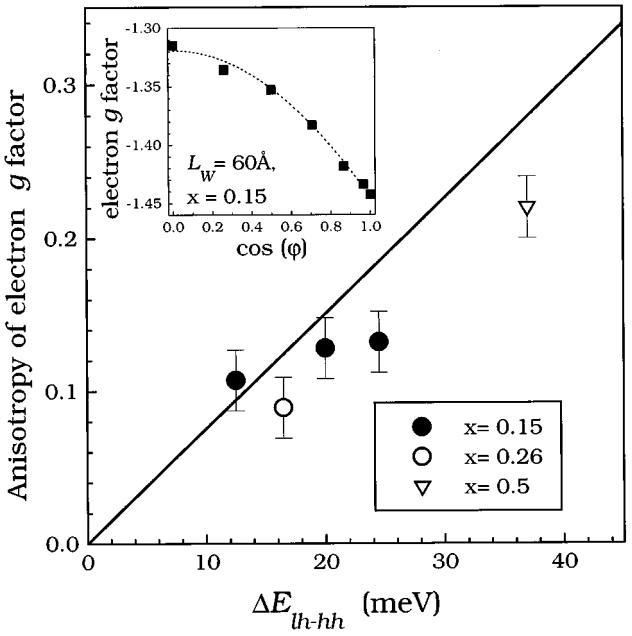

FIG. 6. Correlation between the electron g factor anisotropy Δg and the splitting between light-hole and heavy-hole states $\Delta E_{\text{lh-hh}}$ for the structures with different QW widths and Mg content in the barriers x. The solid line represents a two-band $\mathbf{k}\cdot\mathbf{p}$ calculation according to Eq. (4) with the band parameter E_P of bulk CdTe and with a fixed energy of the heavy-hole exciton transition: $E_{\text{ex}}=1.65$ eV. The inset depicts the anisotropic behavior of the electron g factor in a 60 Å SQW. The dashed line shows a fit with Eq. (2) which yields $g_{\parallel}^{e}=-1.44$ and $g_{\perp}^{e}=-1.32$.

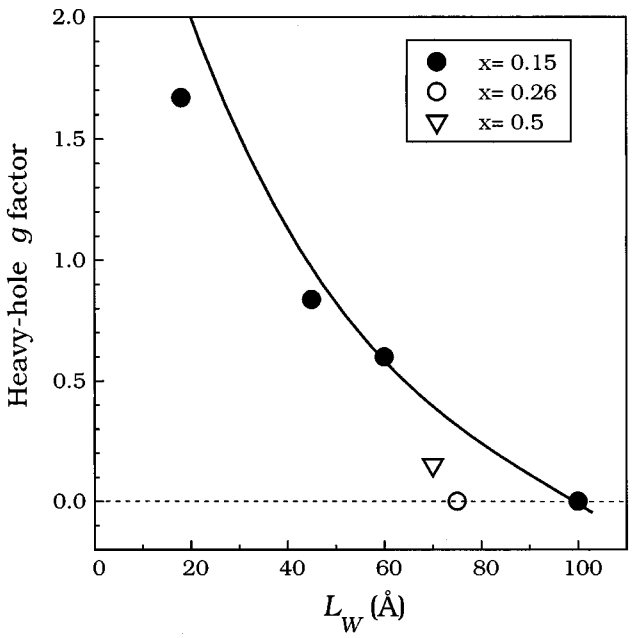

FIG. 7. Dependence of the longitudinal component of the heavy-hole g factor $g_{\parallel}^{\text{hh}}$ on the QW width L_W. The solid line shows results of the calculations from Ref. 6 for $CdTe/Cd_{0.7}Mg_{0.3}Te$ SQW's with the valence band parameter $\kappa=-1.57$.

$$\Delta g \approx \frac{E_P}{E_{\text{ex}}^2}\Delta E_{\text{lh-hh}}, \tag{4}$$

calculated with a fixed value of $E_{\text{ex}}=1.65$ eV and the band parameter $E_P=21.0$ eV of bulk CdTe. It can be seen from Eq. (4) that the sign of Δg is determined by the relative position of the light- and heavy hole subbands: Δg is positive if the ground state in the valence band is the heavy-hole.

Now we turn our attention to the strongly anisotropic heavy-hole g factor. The longitudinal component of the heavy-hole g factor increases while L_W decreases. This dependence is shown in Figure 7. In the first approximation $g_{\parallel}^{\text{hh}}$ is determined by the valence band parameter κ ($g_{\parallel}^{\text{hh}}\approx -6\kappa$), which in turn depends on the energy gap of zinc-blende semiconductors [see Eq. (9) in Ref. 30]. This explains qualitatively the tendency in the variation of $g_{\parallel}^{\text{hh}}$ with L_W, but gives no quantitative agreement. We thus compare our experimental data with the result of precise calculations from Ref. 6 performed in a multiband envelope-function appoximation for $CdTe/Cd_{0.7}Mg_{0.3}Te$ QW's. The theoretical dependence is shown by the solid line in Fig. 7. The good agreement between this result and the experimental data is obtained for the the value of the valence band parameter $\kappa=-1.57$ and renormalized for QW's from its value in bulk CdTe ($\kappa=0.35$).[31] The difference in the Mg content in the barriers ($x=0.3$ in the calculations and $x=0.15$, 0.26, and 0.5 for our samples) should not strongly affect the results since the penetration of the heavy-hole wave function in the barrier is not significant. The measured transverse components of the heavy-hole g factor are negligibly small for all samples: $|g_{\perp}^{\text{hh}}|<0.04$. In zinc-blende semiconductors this value is determined by the valence band parameter q which is usually close to zero.[30,31]

IV. CONCLUSIONS

We have measured the electron, exciton, and heavy-hole g factors in $CdTe/Cd_{1-x}Mg_xTe$ SQW's and some $Cd_{1-x}Mg_xTe$ alloys with a high accuracy by resonant SFRS. The variations of g^e in SQW's are basicaly determined by the changes in the energy gap due to confinement. The anisotropy of the electron g factor correlates with the splitting between light- and heavy-hole exciton states. The results agree with simple expressions derived from $\mathbf{k}\cdot\mathbf{p}$ theory. More elaborate calculations of g^e, taking into account the complicated structure of the ''confined'' valence-band and the penetration of the electron wavefunction into the barrier, should give a still better description of the experimentally observed dependences. The values of the heavy-hole g factor are in good agreement with the calculations of Ref. 6 using a value of the valence-band parameter $\kappa=-1.57$.

ACKNOWLEDGMENTS

The authors are grateful to E. L. Ivchenko, A. A. Kiselev, and M. Oestreich for valuable discussions, and to V. I. Belitsky and R. Henn for a careful reading of the manuscript. Thanks are due to S. Birtel, P. Hieβl, H. Hirt, and M. Siemers for their help. A. A. Sirenko would like to thank the Alexander von Humboldt Foundation for financial support. This work has been supported in part by the Deutsche Forschungsgemeinschaft through SFB 410.

*On leave from A. F. Ioffe Physical Technical Institute, 194021 St. Petersburg, Russia.

[1] M. Cardona, N. E. Christensen, and G. Fasol, Phys. Rev. B **38**, 1806 (1988), and references therein.

[2] M. Willatzen, M. Cardona, and N. E. Christensen, Phys. Rev. B **51**, 17 992 (1995) and references therein.

[3] *Optical Orientation*, edited by F. Meier and B. P. Zakharchenya (North-Holland, Amsterdam, 1984).

[4] B. C. Cavenet, Adv. Phys. **30**, 475 (1981).

[5] E. L. Ivchenko and A. A. Kiselev, Fiz. Tekhn. Poluprovodn. **26**, 1471 (1992) [Sov. Phys. Semicond. **26**, 827 (1992)].

[6] A. A. Kiselev and L. V. Moiseev, Fiz. Tverd. Tela (Leningrad) **38**, 1574 (1996) [Phys. Solid State **38**, 866 (1996)].

[7] V. K. Kalevich and V. L. Korenev, Pis'ma Zh. Eksp. Teor. Fiz. **57**, 557 (1993) [JETP Lett. **57**, 571 (1993)].

[8] E. L. Ivchenko, A. A. Kiselev, and M. Willander, Solid State Commun. **102**, 375 (1997).

[9] M. J. Snelling, E. Blackwood, C. J. McDonagh, R. T. Harley, and C. T. B. Foxon, Phys. Rev. B **45**, 3922 (1992), and references therein.

[10] B. Kowalski, P. Omling, B. K. Meyer, D. M. Hofmann, C. Wetzel, V. Härle, F. Scholz, and P. Sobkowicz, Phys. Rev. B **49**, 14 786 (1994).

[11] E. L. Ivchenko, V. P. Kochereshko, I. N. Uraltsev, and D. R. Yakovlev, in *High Magnetic Fields in Semiconductor Physics III*, edited by G. Landwehr, Springer Series in Solid-State Science Vol. 101 (Springer, Berlin, 1992), p. 533.

[12] V. K. Kalevich and V. L. Korenev, Pis'ma Zh. Éksp. Teor. Fiz. **56**, 257 (1992) [JETP Lett. **56**, 253 (1992)].

[13] V. K. Kalevich, B. P. Zakharchenya, and O. M. Fedorova, Fiz. Tverd. Tela **37**, 287 (1995) [Phys. Solid State **37**, 154 (1995)].

[14] A. A. Sirenko, T. Ruf, K. Eberl, M. Cardona, A. A. Kiselev, E. L. Ivchenko, and K. Ploog, in *Proceedings of the 12th Internation Conference on the Application of High Magnetic Fields in Semiconductor Physics, Würzburg 1996*, edited by G. Landwehr and W. Ossau (World Scientific, Singapore, 1997) (to be published).

[15] Q. X. Zhao, M. Oestreich, and N. Magnea, Appl. Phys. Lett. **69**, 3704 (1996).

[16] V. F. Sapega, M. Cardona, K. Ploog, E. L. Ivchenko, and D. N. Mirlin, Phys. Rev. B **45**, 4320 (1992).

[17] D. N. Mirlin and A. A. Sirenko, Fiz. Tverd. Tela **34**, 205 (1992) [Sov. Phys. Solid State **34**, 108 (1992)].

[18] V. F. Sapega, T. Ruf, M. Cardona, K. Ploog, E. L. Ivchenko, and D. N. Mirlin, Phys. Rev. B **50**, 2510 (1994).

[19] A. A. Sirenko, T. Ruf, N. N. Ledentsov, A. Yu. Egorov, P. S. Kop'ev, V. M. Ustinov, and A. E. Zhukov, Solid State Commun. **97**, 169 (1996).

[20] A. A. Sirenko, T. Ruf, A. Kurtenbach, K. Eberl, in *Proceedings of the 23d International Conference on the Physics of Semiconductors*, edited by M. Scheffler and R. Zimmermann (World Scientific, Singapore, 1996), p. 1385.

[21] A. Waag, F. Fischer, T. Litz, B. Kuhn-Heinrich, U. Zehnder, W. Ossau, W. Spahn, H. Heinke, and G. Landwehr, J. Cryst. Growth **138**, 155 (1994).

[22] B. Kuhn-Heinrich, W. Ossau, H. Heinke, F. Fischer, T. Litz, A. Waag, and G. Landwehr, Appl. Phys. Lett. **63**, 2932 (1993).

[23] R. Hellmann, A. Euteneuer, S. G. Hense, J. Feldmann, P. Thomas, E. O. Göbel, D. R. Yakovlev, A. Waag, and G. Landwehr, Phys. Rev. B **51**, 18 053 (1995).

[24] D. R. Yakovlev, V. P. Kochereshko, R. A. Suris, W. Ossau, A. Waag, G. Landwehr, P. C. M. Christianen, and J. C. Maan, in *Proceedings of the 23rd International Conference on the Physics of Semiconductors*, edited by M. Scheffler and R. Zimmermann (World Scientific, Singapore, 1996), p. 2071.

[25] W. Ossau, B. Jäkel, E. Bangert, and G. Weimann, in *Properties of Impurity States in Superlattice Semiconductors*, Vol. 183 of *NATO Advanced Study Institute, Series B: Physics*, edited by C. Y. Fong, I. P. Batra, and S. Ciraci (Plenum Press, New York, 1988), p. 285.

[26] M. Oestreich, S. Hallstein, A. P. Heberle, K. Eberl, E. Bauser, and W. W. Rühle, Phys. Rev. B **53**, 7911 (1996).

[27] C. Weisbuch and C. Hermann, Phys. Rev. B **15**, 816 (1977).

[28] C. Hermann and C. Weisbuch, Phys. Rev. B **15**, 823 (1977).

[29] In principle, stress-induced *in-plane* mixing of the light- and heavy-hole states can change significantly both components of the hole g factor, but this is not the case for our system.

[30] P. Pfeffer and W. Zawadzki, Phys. Rev. B **53**, 12 813 (1996).

[31] Ch. Neumann, A. Nöthe, and N. O. Lipari, **37**, 922 (1988).